

COMPARISON OF UNFOLDING CODES FOR NEUTRON SPECTROMETRY WITH BONNER SPHERES

S. Barros^{1,*}, V. Mares², R. Bedogni³, M. Reginatto⁴, A. Esposito³, I. F. Gonçalves¹, P. Vaz¹ and W. Rühm²

¹Instituto Superior Técnico, CTN, Estrada Nacional 10 (ao km 139,7), Bobadela LRS 2695-066, Portugal

²Helmholtz Zentrum München, HMGU, Ingolstädter Landstraße 1, Neuherberg D-85764, Germany

³Istituto Nazionale di Fisica Nucleare, Via E. Fermi, 40, Frascati (Roma) 00044, Italy

⁴Physikalisch-Technische Bundesanstalt, Braunschweig D-38116, Germany

*Corresponding author: silviabarros@ctn.ist.utl.pt

This work compares the results of four different unfolding codes, MSANDB, MAXED, FRUIT and BONMA, which are based on different unfolding techniques. Additionally, Bayesian parameter estimation is also considered. All unfolding codes were supplied with the same set of input data acquired at the Environmental Research Station ‘Schneefernerhaus’ on the Zugspitze mountain, corresponding to continuous measurements of secondary neutrons from cosmic radiation. The HMGU high-energy extended Bonner sphere spectrometer (BSS), consisting of 16 measuring channels with ³He proportional counters, was used as a reference BSS. The differences in the neutron spectra obtained with the different unfolding codes are discussed, and the uncertainties of integral quantities, like neutron fluence and ambient dose equivalent, are quantified.

INTRODUCTION

The Bonner sphere spectrometer (BSS)⁽¹⁾ is a neutron spectrometer that is widely used for radiation protection purposes due to a number of advantages like wide energy range, isotropic response, reliable values of neutron fluence and ambient dose equivalent. Using a BSS requires a well-established and validated response function for each sphere, defined as the reading per unit fluence as a function of neutron energy, usually calculated using Monte Carlo (MC) codes and validated with calibration measurements. The most complex aspect of neutron spectrometry with a BSS is the unfolding process, due to the non-uniqueness of the solution. Neutron spectrum unfolding from BSS readings is described by a system of Fredholm integral equations of the first kind. The count rate measured by the *j*th Bonner sphere, C_j , is given by Equation (1), where $R_j(E)$ is the response function of the *j*th sphere and $\Phi(E)$ the neutron fluence to which the system is exposed.

$$C_j = \int_{E_{\min}}^{E_{\max}} R_j(E)\Phi(E)dE \quad j = 1, 2, \dots, M \quad (1)$$

To obtain a numerical solution, the system of Equation (1) is usually written in terms of a discrete system of equations, described by Equation (2), where $R_j(E_k)$ is the response function of the *j*th sphere to neutrons of the energy that corresponds to the *k*th energy bin, *N* the number of energy bins and $\Phi(E_k)$ the fluence in the *k*th energy bin. However, Equation (2) has no unique solution, because the number of unknowns ($N=130$ energy bins of fluence $\Phi(E)$) is much larger than the number of equations ($M=16$

measuring channels), i.e. $N \gg M$.

$$C_j = \sum_{k=1}^N R_j(E_k)\Phi(E_k) \quad j = 1, 2, \dots, M \quad (2)$$

Obtaining accurate results from a BSS is strictly related to the availability of a well-established response matrix (calculated on a consistent number of energy bins and verified in reference neutron fields). In addition, attention must be paid to the correct use of the unfolding code.

There are a number of unfolding codes based on different approaches to determine the $\Phi(E)$ values that satisfy the system of equations described by Equation 2. For example, methods based on linear and non-linear least-squares methods⁽²⁾, Bayesian methods⁽³⁾, maximum entropy⁽⁴⁾ and artificial neural networks⁽⁵⁾, among others⁽⁶⁾, have been used.

The unfolding of the fluence spectrum measured by means of a BSS is associated with several uncertainties from different sources, such as those associated with the measurements, detector's calibration and response functions, which should be analysed and quantified. For example, the effect of using different response functions in the unfolding was previously studied⁽⁷⁾.

Since the unfolding process is an under-determined problem, it must be necessarily provided with some amount of pre-information in addition to the response matrix, the sphere counts and their uncertainties. The use of an initial spectrum which is iteratively varied according to the numerical values of the sphere counts and their uncertainties is a way to provide pre-information. Another way is to parameterise the spectrum as a combination of continuous

functions fully described by a limited number (less than 10) of physically meaningful parameters. Thus, the many available unfolding codes are different in the sense that they differently provide pre-information and differently 'weight' the pre-information, the sphere counts and their uncertainties. Whilst these differences are not likely to seriously affect the spectrum-integrated quantities (total neutron fluence and ambient dose equivalent), they certainly can affect the spectrum shape. So, it is of major importance to compare the results from different codes, using the same count rates and response functions, to understand how the used unfolding method influences the final results.

Some inter-comparison studies were done at the end of 1980s. In the EURADOS inter-comparison^(8,9), 8 institutes participated and 10 unfolding codes were compared. Two BSSs were used: one with eight spheres and another one with four. The maximum neutron energy was around 10 MeV.

In the present study, an inter-comparison among four unfolding codes was performed: MSANDB⁽¹⁰⁾, MAXED⁽⁴⁾, FRUIT⁽¹¹⁾ and BONMA^(12,13) with emphasis on high-energy neutrons (i.e. energies of up to 1 GeV). In addition, the data were analysed using Bayesian parameter estimation using a program developed with the software package WinBugs⁽¹⁴⁾, and this method was regarded as an unfolding code.

MATERIALS AND METHODS

Bonner sphere spectrometer

The HMGU extended-energy BSS used in this study consists of a set of 15 polyethylene (PE) spheres, each

with a spherical ^3He proportional counter in its centre, plus a proportional counter without any moderating sphere (the bare detector). The counters (Centronic Ltd type SP9) have a diameter of 3.3 cm and a partial pressure of 172 kPa. Thirteen of the spheres are pure PE with diameters of 2.5, 3.0, 4.0, 5.0, 5.5, 6.0, 7.0, 8.0, 9.0, 10.0, 11.0, 12.0 and 15.0 inches (although inches are not SI units, Bonner sphere dimensions are traditionally given in this unit: 1 inch=25.4 mm). To increase the response to neutrons with energies above ~ 10 MeV^(15,16), two additional 9-inch PE spheres each have an embedded lead shell, one 0.5 inches in thickness and the other 1.0 inch.

Measurements workplace

The count rates used in this intercomparison were acquired at the Environmental Research Station (UFS) 'Schneefernerhaus' located some 300 m below the Zugspitze summit, corresponding to 2650 m above the sea level (ASL), in Germany. The energy distribution of secondary neutrons from cosmic radiation is continuously monitored by means of a high-energy extended BSS⁽¹⁷⁾. The spectrometer has an hourly time resolution and the daily average of the data acquired on the 16th of December 2012 was used for the unfolding comparison. In Figure 1, the obtained count rates are shown.

Unfolding codes

MSANDB

The MSANDB unfolding code is based on the early SAND-II code⁽¹⁸⁾. MSANDB uses iterative

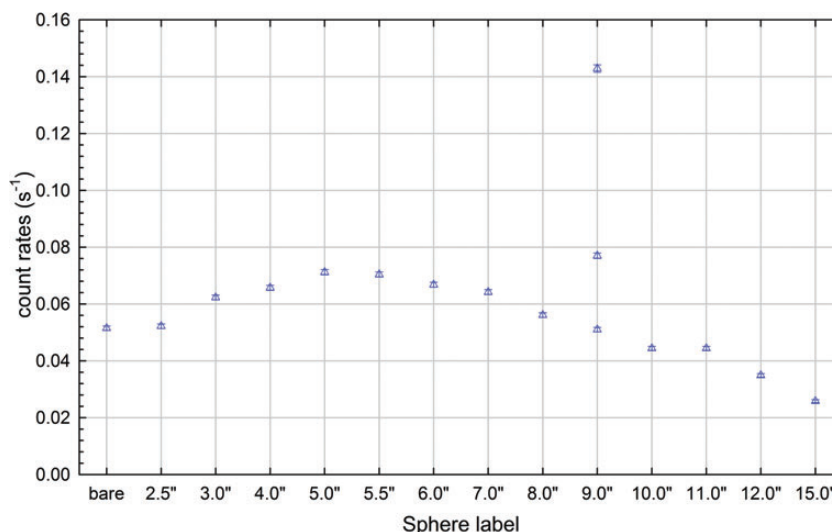


Figure 1. Count rates obtained at UFS on the Zugspitze mountain at 2650-m ASL on the 16th of December 2012.

procedures and requires a start (guess, *a priori*) spectrum containing physical information about the neutron field. The ‘Hybrid8’ start spectrum⁽¹⁹⁾ was used. It represents a rough shape of the expected neutron spectrum, containing four regions: a thermal peak, a flat region of epithermal neutrons, an evaporation peak at 2 MeV and a cascade peak at 100 MeV. The code iteratively modifies the start spectrum to be consistent with the measured count rates of the detectors until a final solution is found. Based on long-lasting experience, 300 iteration steps were used. For more details see Simmer *et al.*⁽¹⁹⁾.

FRUIT

The FRUIT (FRascati Unfolding Interactive Tool) parametric code^(11,20) was designed as a tool for operational measurements in scenarios where very scarce pre-information is available. Besides the sphere response functions, the counts and related uncertainties, FRUIT only requires to introduce qualitative information on the type of ‘radiation environment’ on the basis of a check-box input section. The quantities involved in the unfolding process and their variation are continuously displayed during the convergence process: the plot of the spectrum, the measured and unfolded Bonner sphere counts, the parameters, the tolerances and the doses. The code includes a statistics tool to derive the probability distributions of all quantities related to the final spectrum: the parameters, the fluence (and fractions of fluence in given energy intervals), the ambient dose equivalent and the neutron spectrum, specified bin by bin. Uncertainties are derived on this basis. As an alternative to the parametric approach, FRUIT also includes a ‘guess-spectrum’ unfolding option, based on a special gradient method (SGM). In this work the parametric algorithm has been employed.

BONMA

BONMA v. 167 is a modified version of BON94⁽¹³⁾. This code is based on a parameterisation and on an iterative method. The parameterisation algorithm constructs the initial spectrum which is used as *a priori* information in the iterative procedure. Additionally, a selection of the initial spectrum by the user is also possible. In this work, the parameterised option (Opt. High) was chosen, in which the spectrum is constructed according to empirical physical models. The uncertainties of the calculated spectra bin-per-bin and of integral dosimetric values are estimated using MC methods.

Bayesian parameter estimation

Bayesian parameter estimation is a probabilistic approach for the analysis of data⁽³⁾. The procedure used here follows closely the approach described in ref.

(21). The parameterised spectrum used for the analysis consists of four components: a thermal peak, an intermediate region, a medium energy peak and a high-energy peak. The likelihood function takes into account that the data can be modelled by normal distributions. The choice of prior distributions is determined, as in ref. (21), by the prior information available. The posterior probability distribution, which is the main result of the analysis, is used to estimate the solution spectrum and integral quantities of interest.

MAXED

MAXED is an unfolding code which, given a default spectrum (i.e. an initial estimate of the spectrum), selects a solution spectrum using the maximum entropy principle^(3,4). The default spectrum used for the unfolding with MAXED was the spectrum estimated using Bayesian parameter estimation (described above).

Response function

The response function HEMA99^(16,22) used for the HMGU BSS system was calculated using MCNP (MC Neutron and Photon transport code system⁽²³⁾) for energies <20 MeV and HMCNP (a modified version of MCNP) and LAHET (Los Alamos High-Energy Transport code⁽²⁴⁾) for energies >20 MeV. The response was calculated as the number of absorptions due to ${}^3\text{He}(n, p){}^3\text{H}$ reactions in the ${}^3\text{He}$ proportional detector per incident neutron fluence. Afterwards, the MC calculated response data were interpolated in the energy range between 1 meV and 10 GeV, with 130 logarithmically equidistant energy bins, i.e. 10 bins per decade.

$H^*(10)$ conversion coefficients

The neutron energy spectra were folded with fluence-to-dose conversion coefficients to estimate the neutron ambient dose equivalent. A combination of the conversion coefficients from International Commission on Radiological Protection 74⁽²⁵⁾ extended to high energies with data from Pelliccioni⁽²⁶⁾ was used.

Measurements with extended REM counter

A high-energy extended Andersson–Braun REM counter (NM500X manufactured by Münchener Apparatebau für elektronische Geräte GmbH)⁽²⁷⁾ is continuously acquiring hourly $H^*(10)$ data at UFS. The measured daily average of the equivalent dose rate on the 16th of December 2012 was 17.81 ± 2.3 pSv h⁻¹.

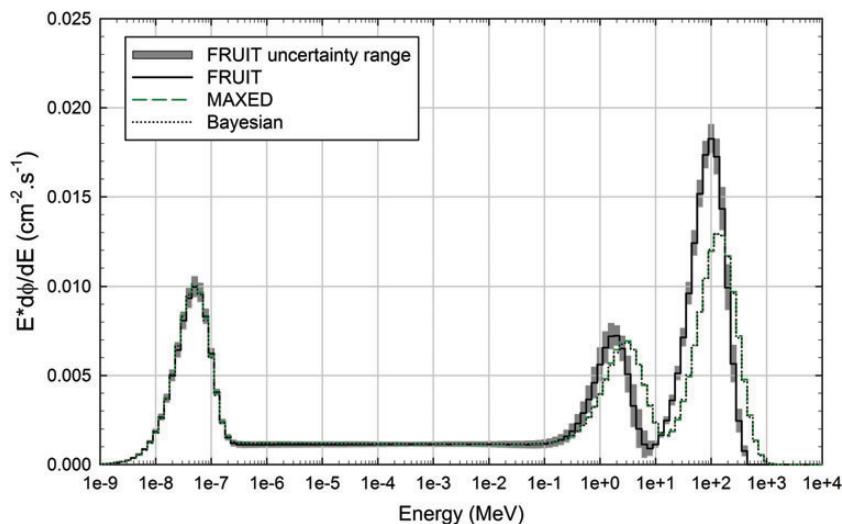


Figure 2. Unfolded neutron spectra obtained with FRUIT, MAXED and Bayesian methods for the data obtained on the 16th of December 2012.

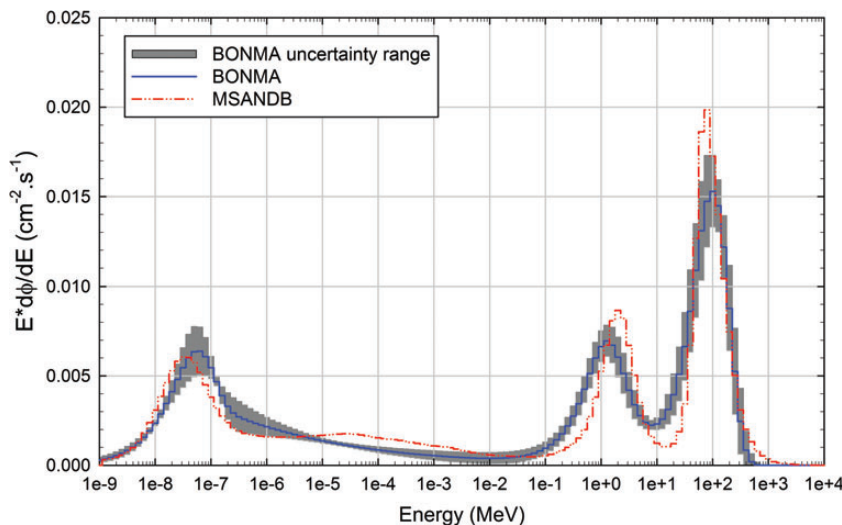


Figure 3. Unfolded neutron spectra obtained with BONMA and MSANDB for the data obtained on the 16th of December 2012.

RESULTS AND DISCUSSION

Unfolded neutron spectrum

Figures 2 and 3 show the neutron spectra obtained with the different unfolding codes, for the 16th of December 2012 daily data. The FRUIT and BONMA bin-per-bin uncertainties are shown in grey.

A comparison of the results shows that all the spectra have similar shape. It is worth noting that the

spectra obtained with MAXED and Bayesian parameter estimation are almost identical. The reason for this is that the Bayesian estimate of the neutron spectrum already fits the data so well that MAXED only makes small corrections to the default spectrum. Slight discrepancies in the position and height of thermal, evaporation and cascade peaks (see Figures 2 and 3) could be attributed to different unfolding methods used. The MAXED and

Table 1. Integral fluence values obtained with the different unfolding codes, with the corresponding uncertainties (1σ), and comparison to the MSANDB results. Th.+Epi. corresponds to the sum of thermal and epithermal energy regions; Ev.+Casc. corresponds to the sum of evaporation and cascade energy regions.

	Th.+Epi. ($\text{cm}^{-2} \text{s}^{-1}$)	Deviation to MSANDB	Ev.+Casc. ($\text{cm}^{-2} \text{s}^{-1}$)	Deviation to MSANDB	Total ($\text{cm}^{-2} \text{s}^{-1}$)	Deviation to MSANDB
FRUIT	$3.38\text{E}-2 \pm 4.22\text{E}-4$	1.03 ± 0.03	$4.85\text{E}-2 \pm 9.95\text{E}-4$	1.05 ± 0.03	$8.23\text{E}-2 \pm 1.08\text{E}-3$	1.04 ± 0.03
BONMA	$3.13\text{E}-2 \pm 9.80\text{E}-4$	0.95 ± 0.04	$4.85\text{E}-2 \pm 1.93\text{E}-3$	1.05 ± 0.05	$7.85\text{E}-2 \pm 2.16\text{E}-3$	0.99 ± 0.04
MSANDB	$3.29\text{E}-2 \pm 7.00\text{E}-4$	—	$4.63\text{E}-2 \pm 1.02\text{E}-3$	—	$7.92\text{E}-2 \pm 2.38\text{E}-3$	—
MAXED	$3.46\text{E}-2 \pm 4.44\text{E}-4$	1.05 ± 0.03	$4.41\text{E}-2 \pm 6.56\text{E}-4$	0.95 ± 0.03	$7.87\text{E}-2 \pm 5.49\text{E}-4$	0.99 ± 0.03
Bayesian	$3.44\text{E}-2 \pm 1.39\text{E}-3$	1.05 ± 0.05	$4.44\text{E}-2 \pm 4.00\text{E}-3$	0.96 ± 0.09	$7.87\text{E}-2 \pm 3.03\text{E}-3$	0.99 ± 0.05

Table 2. Ambient dose equivalent rates obtained with the different unfolding codes, with the corresponding uncertainties (1σ), and comparison with the MSANDB results. Th.+Epi. corresponds to the sum of the thermal and epithermal energy regions; Ev.+Casc. corresponds to the sum of the evaporation and cascade energy regions.

	Th.+Epi. (pSv s^{-1})	Deviation to MSANDB	Ev.+Casc. (pSv s^{-1})	Deviation to MSANDB	Total (pSv s^{-1})	Deviation to MSANDB
FRUIT	0.43 ± 0.01	1.12 ± 0.03	17.50 ± 0.36	1.05 ± 0.03	17.92 ± 0.24	1.05 ± 0.03
BONMA	0.39 ± 0.01	1.03 ± 0.04	17.17 ± 0.70	1.03 ± 0.05	17.51 ± 0.48	1.03 ± 0.05
MSANDB	0.38 ± 0.01	—	16.62 ± 0.36	—	17.00 ± 0.51	—
MAXED	0.44 ± 0.01	1.15 ± 0.03	15.27 ± 0.23	0.92 ± 0.02	15.70 ± 0.18	0.92 ± 0.03
Bayesian	0.44 ± 0.03	1.15 ± 0.07	15.20 ± 1.76	0.91 ± 0.11	15.60 ± 1.49	0.92 ± 0.09

MSANDB evaporation peaks are slightly shifted to higher energies compared with that from FRUIT and BONMA. Also, MAXED cascade peak is shifted to higher energy and its height is rather lower. It should be noted that while the spectra unfolded by different codes may differ somewhat in shape, integral quantities derived from spectra, such as fluence and ambient dose equivalent, are in very good agreement.

Integral values of fluence and ambient dose equivalent rate

Integral neutron fluence rates

In Table 1, where Th.+Epi. corresponds to the sum of thermal and epithermal energy regions and Ev.+Casc. corresponds to the sum of evaporation and cascade energy regions, the integral values of the neutron fluence rates obtained with the different codes are compared with the MSANDB results. The values are compared with this code only because the HMGU BSS system was used for measurements and it is the standard code used to unfold spectra at this institute. Also, the presented uncertainties take into account only the uncertainties associated with the count rates and response function.

One can observe that the maximum deviation between the codes and MSANDB is 5% for the Th.+Epi. and Ev.+Casc. energy group. The total maximum deviation is 4% and the values are in agreement within the uncertainties.

Integral ambient-dose-equivalent rates

Concerning the integral values of the ambient-dose-equivalent rate, shown in Table 2, it can be observed that the deviation in the low-energy region goes up to 15%, but this deviation, in the most significant energy regions for neutron dosimetry (Ev.+Casc.), goes up only to 9%. As in Table 1, the shown uncertainties take into account only the count rates and response function uncertainty.

It is to note that the extended REM counter measurements are validated by the BSS unfolded results, since the values are in agreement.

Measured and calculated count rates

A comparison of the measured and calculated count rates, which are the count rates obtained by folding the response function of each sphere with the unfolded spectrum, is a standard procedure to check the consistency of an unfolded spectrum with the data. In Figure 4 the ratios of the calculated to the measured count rates are presented. The count rates obtained with the different codes are in agreement with each other and, except for the 11-inch sphere, are also in agreement with the measurements, within uncertainties. It should be noticed that the ratio $C_{\text{calc}}/C_{\text{meas}}$ for the 11-inch sphere is ~ 0.9 , which is caused by the slightly higher measured count rate with this sphere (see Figure 1) which is due to an unknown reason.

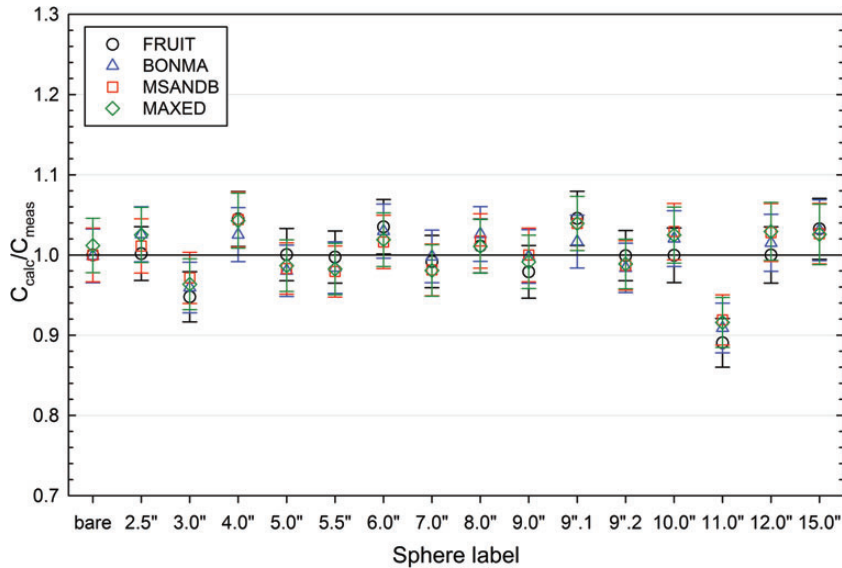


Figure 4. Ratio of calculated and measured count rates.

CONCLUSIONS

Neutron spectrum unfolding from BSS measurements is a challenging task and the correct use of unfolding codes requires experience. Using the same BSS system, the same response functions and the same measured count rates, five different codes were used in this study to derive the neutron spectrum of secondary cosmic neutrons from data measured on the Zugspitze mountain. The shapes of the spectra obtained with the different codes are in agreement, with some slight differences in height and position of the peaks. These differences may be attributed to the start spectrum and to the different unfolding methods used. Concerning the integral quantities of the fluence and ambient dose equivalent rates, the values are in very good agreement and the maximum deviation to the MSANDB values for the Ev.+Casc. energy region is 5 and 9%, for fluence and dose values, respectively. The comparison between the measured and unfolded count rates shows agreement within uncertainties.

FUNDING

S. Barros thank to the support of Fundação para a Ciência e a Tecnologia (FCT) for her fellowship (SFRH/BD/74053/2010).

REFERENCES

1. Bramblett, R. L., Ewing, R. I. and Bonner, T. W. *A new type of neutron spectrometer*. Nucl. Instrum. Methods **9**, 1–12 (1960).
2. Matzke, M. *Propagation of uncertainties in unfolding procedures*. Nucl. Instrum. Methods Phys. Res. A **476**, 230–241 (2002).
3. Sivia, D.S. and Skilling, J. *Data Analysis—A Bayesian Tutorial*. 2nd edn. Oxford University Press (2006)
4. Reginatto, M., Goldhagen, P. and Neumann, S. *Spectrum unfolding, sensitivity analysis and propagation of uncertainties with the maximum entropy deconvolution code MAXED*. Nucl. Instrum. Methods A **476**, 242–246 (2002).
5. Vega-Carrillo, H. R., Hernandez-Dávila, V. M., Manzanares-Acuña, E., Mercado, G. A., Gallego, E., Lorente, A., Perales-Muñoz, W. A. and Robles Rodríguez, J. A. *Artificial neural networks in neutron dosimetry*. Radiat. Prot. Dosim. **118**, 251–259 (2006).
6. Reginatto, M. *Overview of spectral unfolding techniques and uncertainty estimation*. Radiat. Meas. **45**, 1323–1329 (2010).
7. Pioch, C., Mares, V. and Rühm, W. *Influence of Bonner spheres response functions above 20 MeV on unfolded neutron spectra and doses*. Radiat. Meas. **45**, 1263–1267 (2010).
8. Alevra, A. V., Matzke, M. and Siebert, B. R. L. *Experiences from an international unfolding intercomparison with Bonner spheres*. In: Proceedings of the 7th ASTM-EURATOM Symposium on Reactor Dosimetry, Strasbourg (1990).
9. Alevra, A. V. et al. *Unfolding Bonner-Sphere data: a European intercomparison of computer codes*. Physikalisch Technische Bundesamt. Laborbericht PTB-7.22-90-1, Braunschweig (1990).
10. Matzke, M. *Private communication*. Later integrated into the Neutron2: Metrology File NMF-90, available from NEA Databank (1987). <http://www.nea.fr/abs/html/jaea1279.html>.
11. Bedogni, R., Domingo, C., Esposito, A. and Fernandez, F. *FRUIT: an operational tool for multisphere neutron*

COMPARISON OF SPECTRUM UNFOLDING CODES

- spectrometry in workplaces.* Nucl. Instrum. Methods Phys. Res. A **580**, 1301–1309 (2007).
12. Sannikov, A. V., Schraube, G. and Mares, V. Private communication.
 13. Sannikov, A.V. *BON94 code for neutron spectra unfolding from Bonner spectrometer data.* CERN internal report CERN/TIS-RP/IR/94-16 (1994).
 14. Spiegelhalter, D. J., Thomas, A. and Best, N. G. *WinBUGS Version 1.3 User Manual.* MRC Biostatistics Unit. The WinBUGS software information (2000). Available on <http://www.mrc-bsu.cam.ac.uk/bugs>.
 15. Mares, V. and Schraube, H. *High energy neutron spectrometry with Bonner spheres.* In Proceedings of the IRPA-Symposium, Radiation Protection in Neighbouring Countries of Central Eur. Prague, Czech Republic, 8–12 September, pp. 543–547 (1998).
 16. Mares, V., Sannikov, A. and Schraube, H. *The response functions of a 3He-Bonner spectrometer and their experimental verification in high energy neutron fields.* In: Proceedings of the 3rd Specialist Meeting on Shielding Aspects of Accelerators, Targets and Irradiation Facilities, Sendai, Japan, pp. 237–248 (1998).
 17. Leuthold, G., Mares, V., Rühm, W., Weitzenegger, E. and Paretzke, H. G. *Long-term measurements of cosmic ray neutrons by means of a Bonner spectrometer at mountain altitudes—first results.* Radiat. Prot. Dosim. **126**(1–4), 506–511 (2007).
 18. McElroy, W., Berg, S., Crockett, T. and Hawkins, R. *Spectra Unfolding.* Technical report AFWL-TR-67-41. US Air Force Weapons Laboratory (1967).
 19. Simmer, G., Mares, V., Weitzenegger, E. and Rühm, W. *Iterative unfolding for Bonner sphere spectrometers—sensitivity analysis and dose calculation.* Radiat. Meas. **45**, 1–9 (2010).
 20. Bedogni, R., Pelliccioni, M. and Esposito, A. *A parametric model to describe neutron spectra around high-energy electron accelerators and its application in neutron spectrometry with Bonner Spheres.* Nuc. Instrum. Methods A **615**, 78–82 (2010).
 21. Reginatto, M. *What can we learn about the spectrum of high-energy stray neutron fields from Bonner sphere measurements?* Radiat. Meas. **44**, 692–699 (2009).
 22. Mares, V., Schraube, G. and Schraube, H. *Calculated neutron response of a Bonner sphere spectrometer with ³He counter.* Nucl. Instrum. Methods A **307**, 398–412 (1991).
 23. Briesmeister, J. *MCNP—a general Monte Carlo N-Particle Transport Code.* Version 4A. Technical report LA-12625-M. Los Alamos National Laboratory (1993).
 24. Prael, R. and Lichtenstein, H. *User Guide to LCS: the LAHET code system.* Technical report LA-UR-89–3014. Los Alamos National Laboratory (1989).
 25. International Commission on Radiological Protection (ICRP). *Conversion coefficients for use in radiological protection against external radiation.* ICRP Publication 74. Pergmon (1997).
 26. Pelliccioni, M. *Overview of fluence-to-effective dose and fluence-to-ambient dose equivalent conversion coefficients for high energy radiation calculated using the FLUKA code.* Radiat. Prot. Dosim. **88**, 279–297 (2000).
 27. Mares, V., Sannikov, A. V. and Schraube, H. *Response functions of the Andersson-Braun and extended range rem counters for neutron energies from thermal to 10 GeV.* Nucl Instrum Methods A **476**(1–2), 341–346 (2002).